

MOTIVATION

- In observations, **MJO activity is systematically modulated by the phase of the QBO**; i.e., anomalously enhanced and suppressed MJO variability during the easterly and westerly phases of the QBO, respectively (Yoo and Son 2016; Son et al. 2017).
- While studies have proposed plausible mechanisms for the observed MJO-QBO coupling, **it remains largely unknown** how QBO-related temperature and wind anomalies in the upper troposphere and lower stratosphere modulate convective activity associated with the MJO (Martin et al. 2021).
- **One of the proposed ideas** is that the QBO-related **negative temperature anomalies** in the upper troposphere/lower stratosphere during the easterly phase of the QBO (EQBO) can promote stronger MJO convection by **strengthening the cold cap anomalies above the MJO convection** (e.g., Nishimoto and Yoden, 2017; Hendon and Abhik, 2018).
- In this study, we **examine and compare the characteristics of convective systems** between the EQBO and WQBO using satellite observations, reanalysis product, and **cloud-precipitation (hybrid) regimes**, in an attempt to reveal the mechanism through which the QBO affects the MJO.

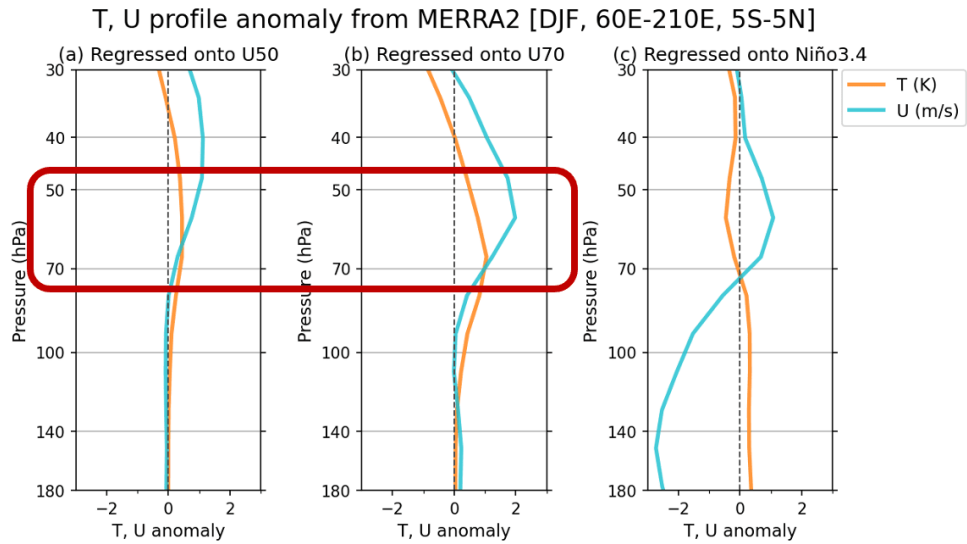
DATA AND METHODOLOGY

1. Cloud and Precipitation data
 1. MODIS C6.1 daily 1-deg Terra and Aqua (Level3)
 1. Cloud top pressure (CTP)
 2. Cloud optical thickness (COT)
 3. Cloud top temperature (CTT)
 4. Joint histogram of CTP and COT
 2. IMERG V06B (Final Run) 30-minutely 0.1-deg precipitation rate
 1. IMERG precipitation is spatio-temporally matched to MODIS data
 3. 2002.12 to 2020.11 (18-years)
2. Cloud-precipitation (hybrid) regime
 1. Cld42-Pr6x1 set: 42 bins of 2D joint histogram of CTP and COT are combined with 6-bin precipitation histogram at 1-deg scale and used for *k*-means clustering, which results in 16 optimized regimes in tropics (see Jin et al. 2021)
 2. Details of regimes are displayed in Supplementary section 1 (right-most top box)
3. Temperature and Zonal wind
 1. Temperature and zonal wind profiles are obtained from MERRA2.
 2. For the values at 50 and 70 hPa, linear interpolation was performed from MERRA2 vertical grid.
4. Calculating energy budget
 1. For the atmospheric radiation budget, CERES Synoptic TOA and surface fluxes and clouds (SYN) 1deg-Level3 product. With hourly data, instantaneous energy budget is obtained by spatio-temporal matching, same way as IMERG precipitation.
 2. Downward radiation is set as positive.
 3. Coefficient to used for transforming precipitation into latent heat is 28.94W/m^2 , following Kato et al. (2016).

RESULT - PART1: CASE SELECTION

1. Temperature profile responding to QBO

1. Profiles regressed onto stratospheric zonal wind (Figure 1)



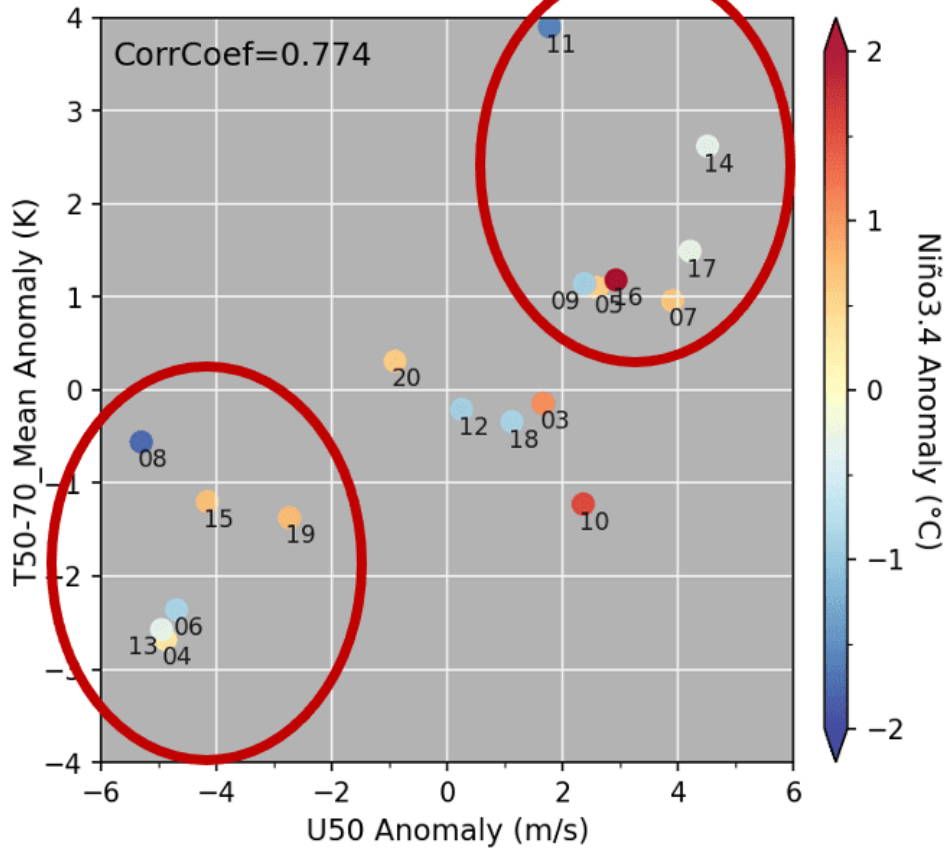
1. Area mean (60-210E, 5S-5N) U and T profile from MERRA2 in Dec to Feb are regressed onto (a) U at 50hPa, (b) U at 70hPa, and (c) Niño3.4 index.

2. **U70** is associated with **larger anomalies of U and T**.

3. We are focusing on **mean T anomaly at 50 and 70hPa** in the following.

2. Temperature anomaly vs. QBO index (U50; Figure 2)

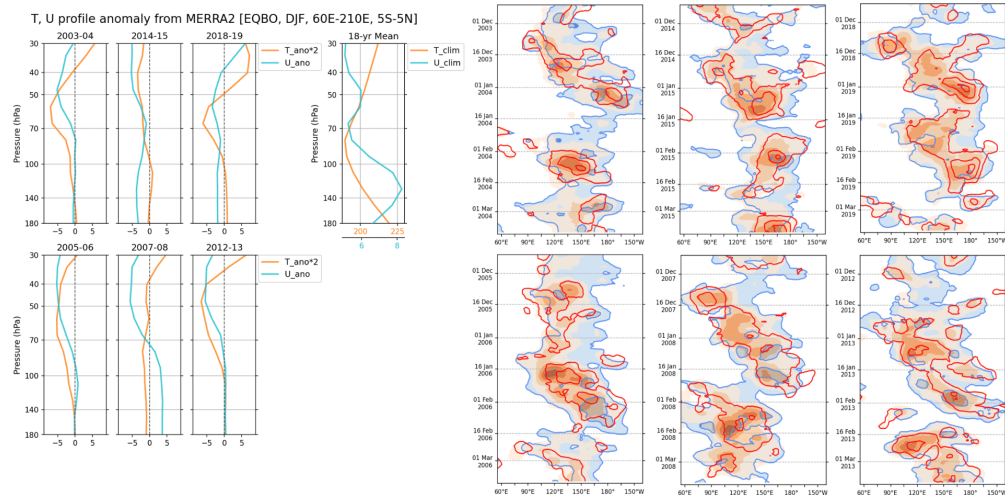
[DJF, 60E-210E, 5S-5N]



1. Mean T anomaly at 50 to 70hPa of each DJF is aligned with U50 anomaly which is commonly used for QBO index, with colors indicating the status of ENSO.
2. They are **positively correlated (coefficient=0.774)**, but with a few outliers.
3. Two groups (red circles) representing EQBO and WQBO are compared.

2. Convective systems by QBO and ENSO conditions

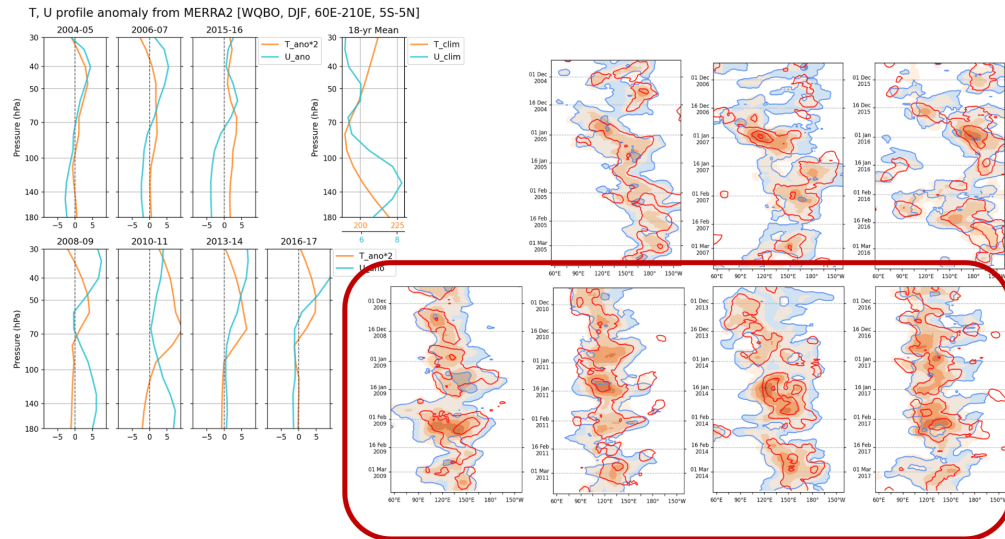
1. EQBO cases (Figure 3)



1. EQBO cases for El Niño years (top) and La Niña years (bottom).

- Left panels show seasonal anomaly of T and U profiles, and right panels show temporal evolution of convective systems (Core: red contour, Anvil: orange color area, and Cirrus: light blue area; details are in right top section of "Regime Details")
- These cases show "USUAL" MJO signature of Eastward propagation.

2. WQBO cases (Figure 4)

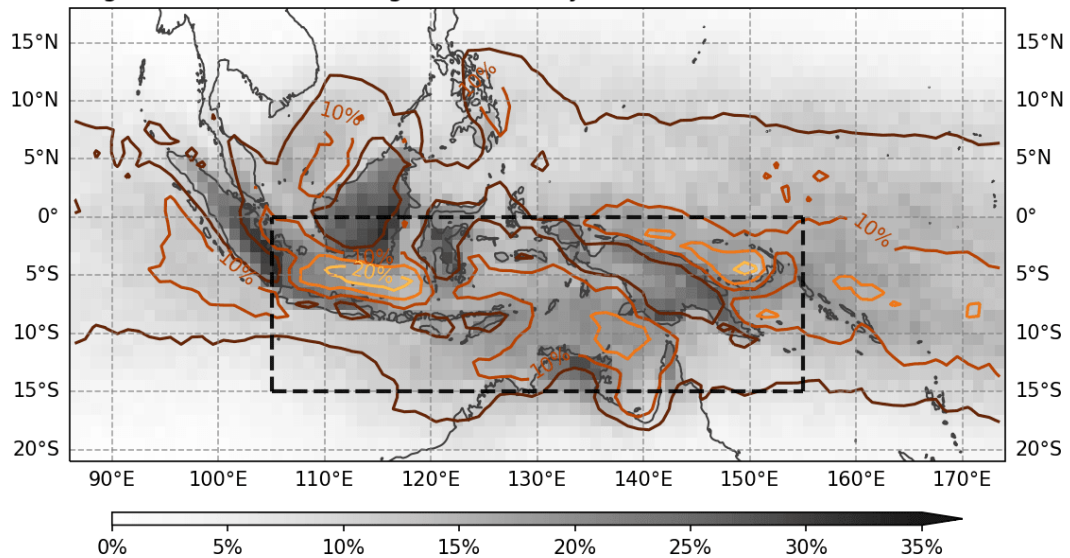


- WQBO cases for El Niño years (top) and La Niña years (bottom).
- Particularly for La Niña years, **positive T anomalies are prominent, and convective systems look "STAGNANT."**

3. Targer area setup (Figure 5)

RFO [Pr6x1_k16, 2003-20 DJF]

Regime1+2: Contour, Regime4+6: Gray



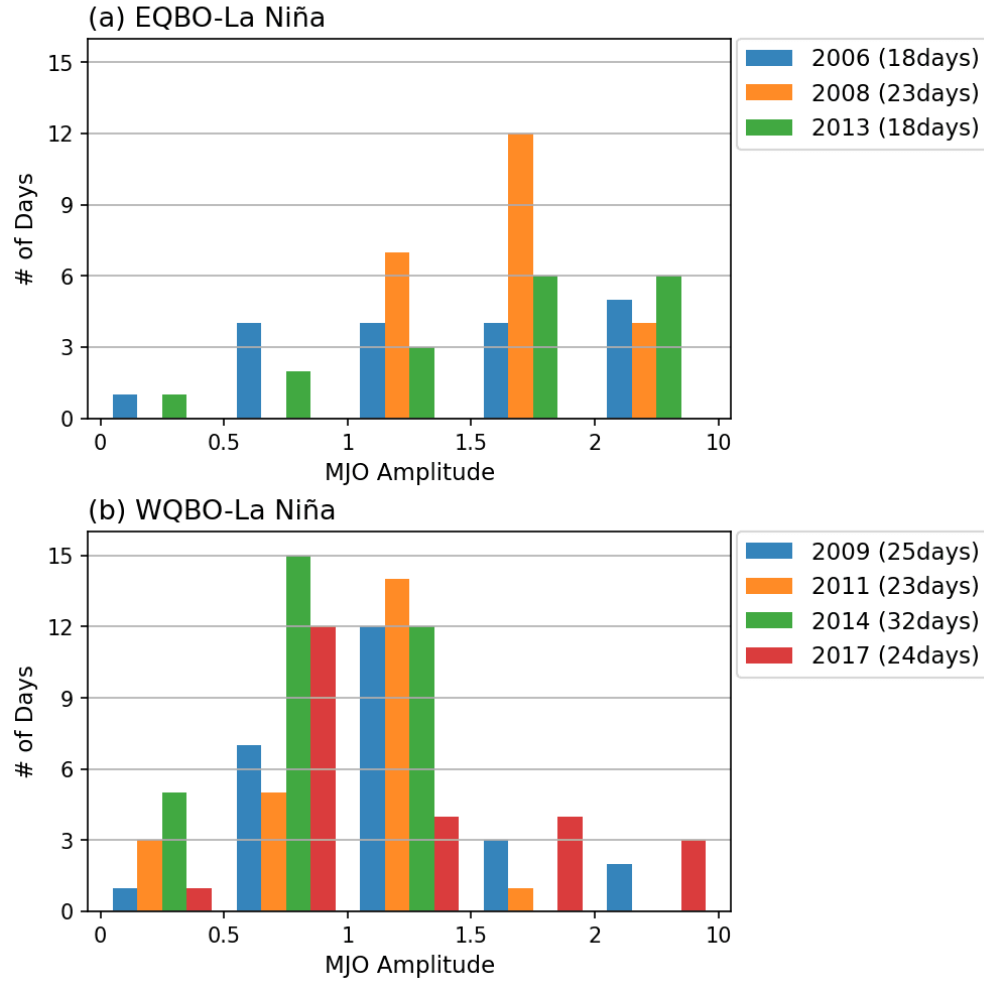
- Dash box (105-155E, 15S-0N; referred to as "Southern Maritime Continent (SMC)")
- Including peak RFO location of Core (Regime 1&2; contour) and Anvil (Regime 4&6; gray color fill; details are in the section of "Regime Details")
- Also considering the location of stagnant convection pattern in WQBO-La Niña cases

RESULT - PART2: KEY DIFFERENCES

1. Occurrence statistics by MJO amplitude

1. **RMM index** is chosen since it reflects not only the convective features of the MJO, but also **the large-scale circulation**.

RMM Phase=4 or 5 in DJF

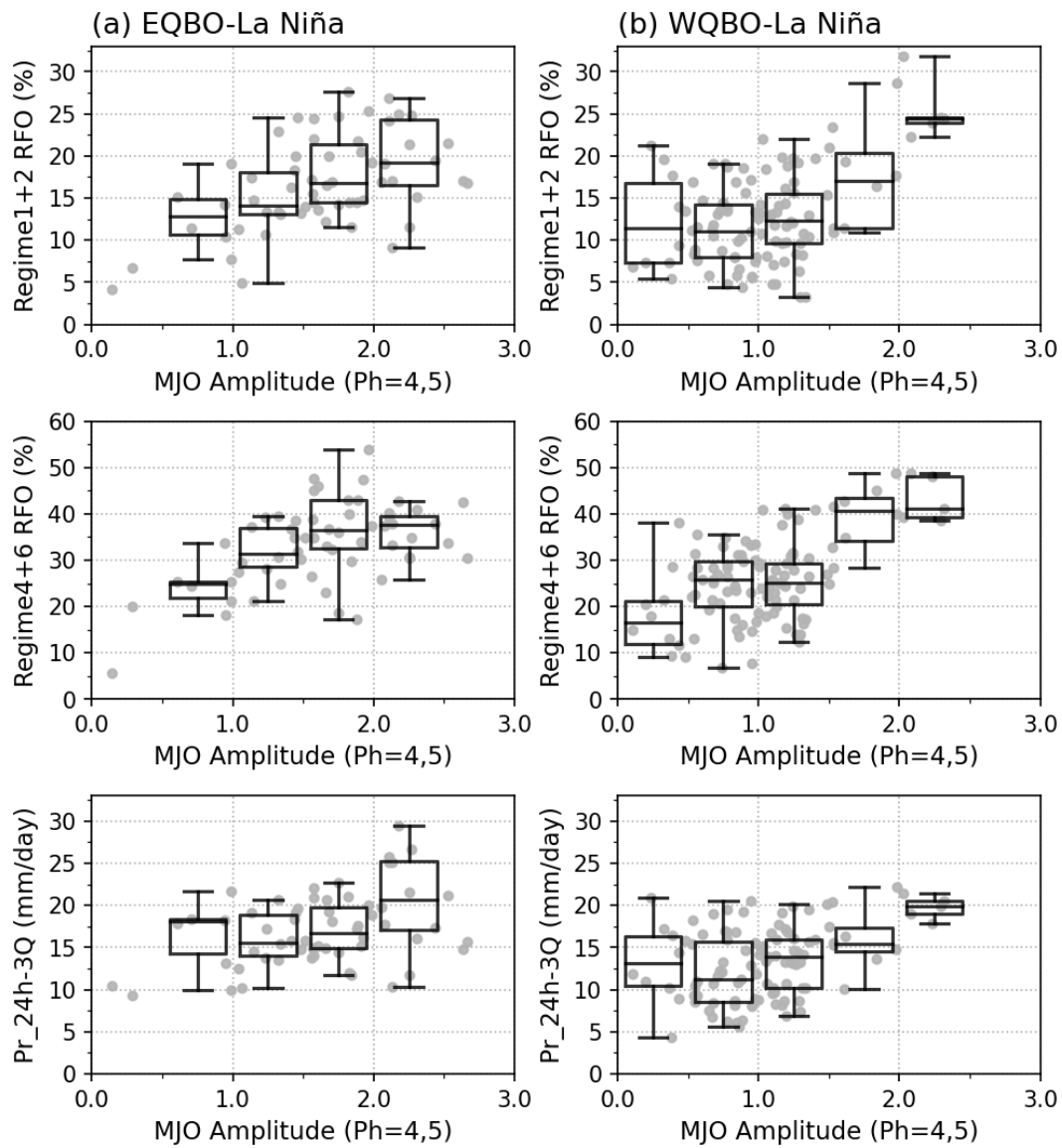


1. (Figure 6) The analysis is limited to **La Niña DJFs** and **MJO phases 4&5**.

2. WQBO cases (bottom) show more MJO days (since stagnant) but with weaker amplitudes.

2. Overview of domain mean values (Figure 7)

Variability by MJO Amplitude [DJF in SMC]



1. In the Southern Maritime Continent (SMC) domain, relative frequency of occurrence (RFO) of convective core (Regime 1&2; top) and anvil (Regime 4&6; middle) parts by MJO amplitudes are compared between EQBO-La Niña (left) and WQBO-La Niña years (right). Bottom panels show 75% percentile (3Q) precipitation rates.

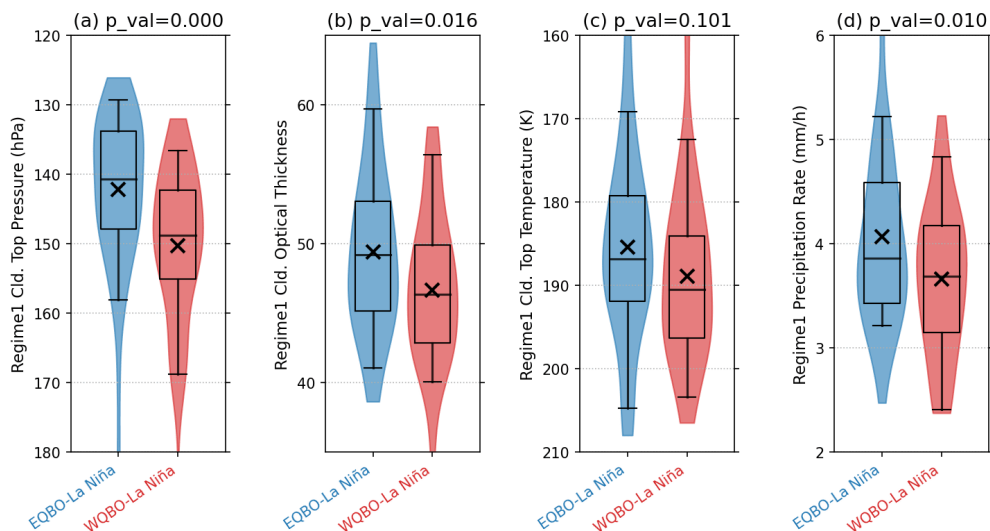
2. For days with similar MJO amplitudes (e.g., 1 to 2), EQBO cases show **more frequent occurrence** of convective **core and a larger anvil area** with **heavier precipitation**.

3. Regime1 properties under similar condition

1. Here, the characteristics of Regime1 representing full of convective core at 1-deg scale are compared under the **same strong MJO condition** by RMM index (Amplitude>1).

2. Cloud properties (Figure 8)

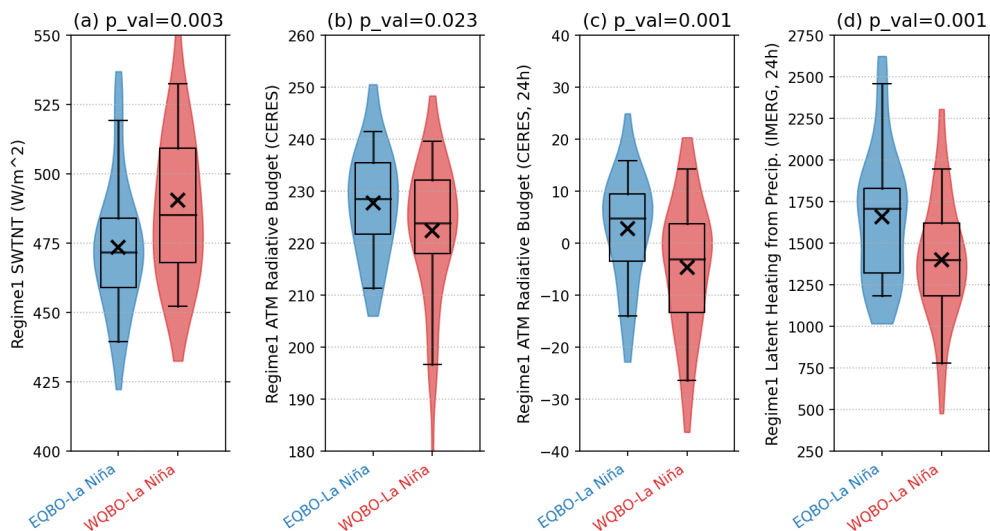
Variability of Regime1 Characteristics [RMM Ph=4+5, Amp>1]



1. The distributions of (a) CTP, (b) COT, (c) CTT, and (d) instantaneous precipitation rate of Regime1 grid cells are shown. "x" mark represents the mean while horizontal bar in the box represents the median.
2. Under a similar MJO and ENSO condition, **EQBO cases show lower CTP and CTT** (higher altitude) and **thicker convective core with heavier precipitation**, although CTT is not significant at the 95% confidence level.

3. Energy budget properties (Figure 9)

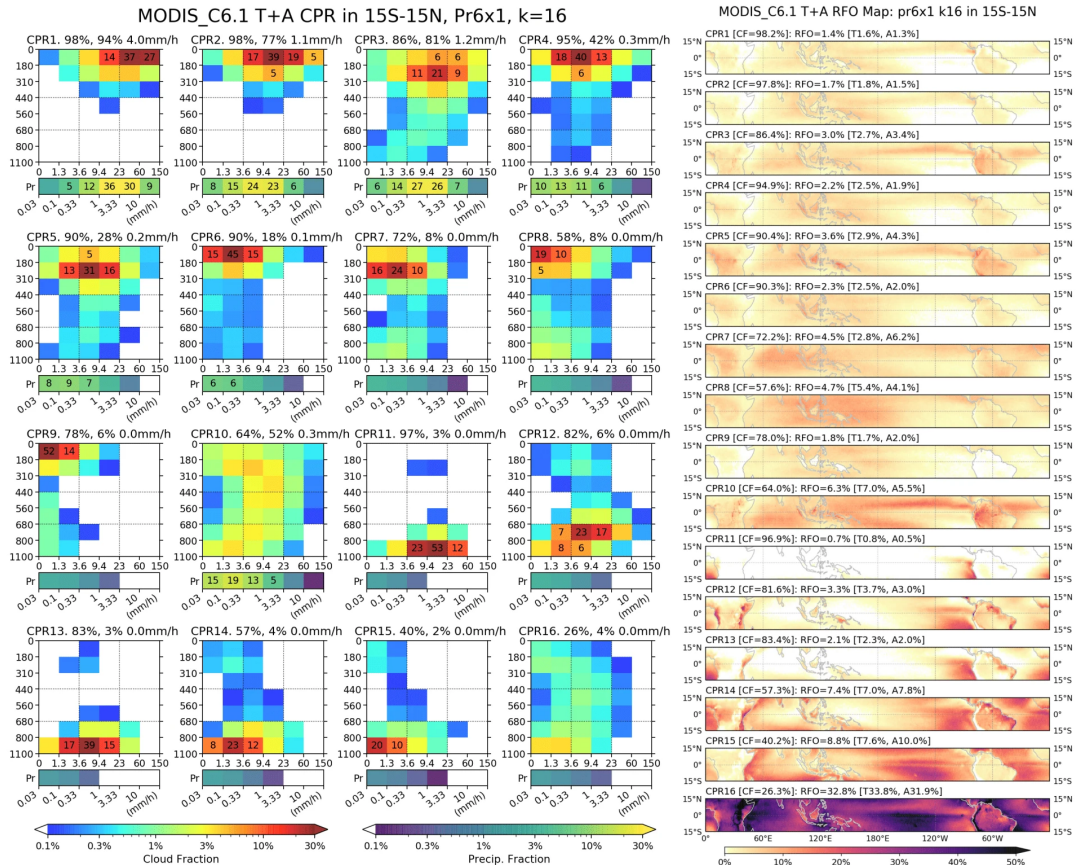
Variability of Regime1 Characteristics [RMM Ph=4+5, Amp>1]



1. The distributions of (a) SWTNT (Downward net SW at TOA), (b) instantaneous atmospheric radiative budget (W/m^2), (c) 24h integrated atmospheric radiative budget (W/m^2), and (d) 24h integrated latent heat (W/m^2) converted from precipitation for Regime1 grid cells.
2. SWTNT is lower in EQBO cases, which is consistent with the lower CTP and CTT (i.e., more reflection).
3. However, atmospheric radiation budget is larger in EQBO cases meaning more LW is absorbed by convective clouds.
4. Considering both the atmospheric radiation budget and latent heat, **atmospheric energy surplus is larger in EQBO cases.**

REGIME DETAILS

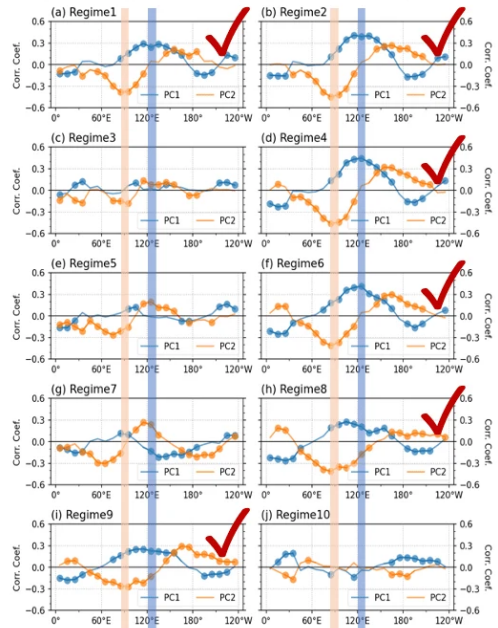
1. Cld42-Pr6x1 set (Figure S1)



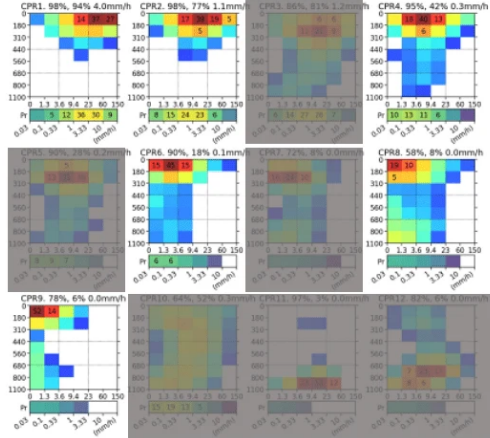
2. Selecting regimes corresponding to MJO

1. Correlation coefficients were calculated between each regime RFO and RMM PC1 (blue) or PC2 (orange) for every 10-deg longitude bins. (Figure S2)

Tamean Pr6x1 k16 RFO vs. RMM PCs Corr. Coef., 2003-20 DJF in 15S-15N



MODIS_C6.1 T+A CPR in 15S-15N, Pr6x1, k=16



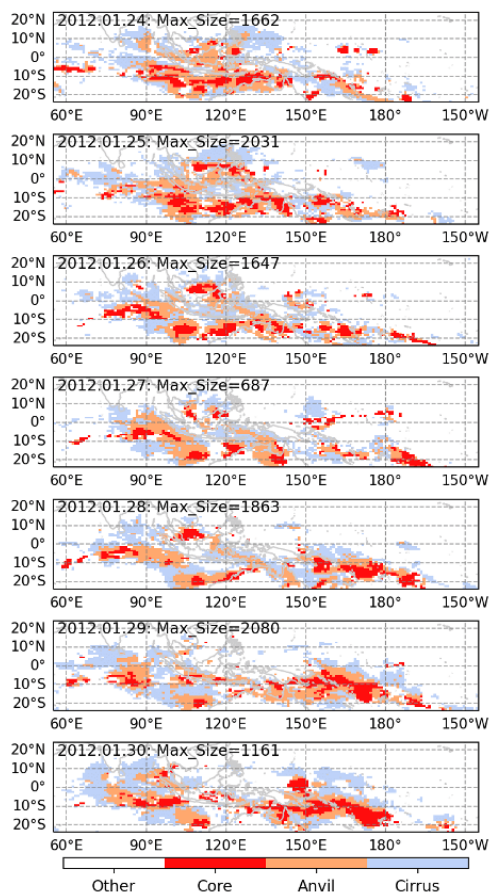
- Regime 1, 2: Core and thick stratiform
- Regime 4, 6: Anvil
- Regime 8, 9: Cirrus

2. Based on correlation patterns with MJO PCs, 6 regimes were selected

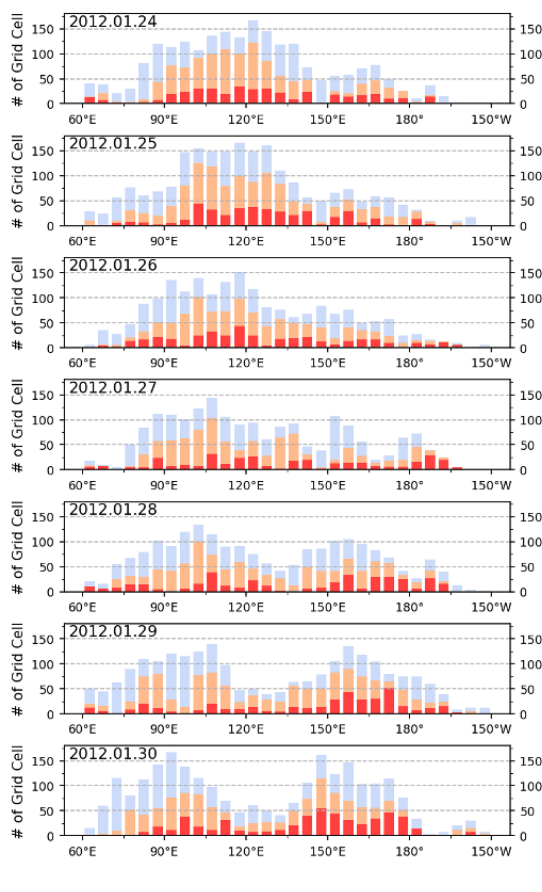
3. These 6 regimes were classified as Core (Regime 1&2), Anvil (Regime 4&6), and Cirrus (Regime 8&9) by the centroid shape.

3. An example of daily evolution (Figure S3)

Aggregate1+2+4+6+8+9 Snapshot [Pr6x1_k16]



Aggregate1+2+4+6+8+9 Snapshot [Pr6x1_k16]



1. Left panels show daily snapshot of convective systems.

2. Right panels show meridional sum of grid cells assigned to Core (red), Anvil (orange), and Cirrus (light blue).

3. Obtained values in right panels constitute the Hovmöller diagram shown in Result - Part1.

SUMMARY AND CONCLUSION

- This study documented the difference in the characteristics of convective systems between EQBO and WQBO years using the cloud-precipitation regimes.
- While other studies have extensively examined the differences in large-scale and MJO-scale anomalies, this study has **focused on individual convective systems embedded in the MJO envelope**.
- We focused on **La Niña years** and the **southern Maritime Continent (SMC) region** because MJO activity shows a clear difference between EQBO and WQBO in this region/time.
- We showed that **convective systems** were **taller** and **optically thicker** with **more number of convection core during EQBO-La Niña DJFs** compared to WQBO-La Niña DJFs.
- Our results suggest that **QBO-associated temperature anomalies in the lower stratosphere affect the MJO** by modulating the morphology and strength of underlying convective systems.
- Our results **likely explain how the large-scale circulation anomalies maintain and further strengthen the MJO**.
- Additionally, it is worthwhile to note that the variability of temperature anomaly in lower stratosphere is slightly inconsistent to QBO proxy (e.g., U50), potentially due to other factors like ENSO.
- Similar comparison for El Niño years shows that contrasts between EQBO and WQBO are much less significant (not shown).

AUTHOR INFORMATION

Daeho Jin (GESTAR II - UMBC / NASA GSFC; Daeho.Jin@NASA.gov)

Daehyun Kim (U. of Washington)

Lazaros Oreopoulos (NASA GSFC)

ABSTRACT

Tropical convective systems that grow larger than $100,000\text{km}^2$ sizes play a significant role in the water cycle and energy budget of the Earth system. Previously, we developed hybrid tropical cloud-precipitation regimes (TCPRs) derived from Moderate Resolution Imaging Spectroradiometer (MODIS) cloud observations and Integrated Multi-satellite Retrievals for GPM (IMERG) precipitation data at a 1° scale, and demonstrated that TCPRs enabled a simple but effective identification of convective systems at the synoptic scale.

The Madden-Julian Oscillation (MJO) is the dominant mode of tropical intraseasonal variability, which is characterized as a planetary-scale envelop of convective clouds that propagates eastward over the Indo-Pacific warm pool. Recent studies showed a statistically robust correlation between the MJO and the quasi-biennial oscillation (QBO); MJO-related convective activities are enhanced and suppressed during an easterly and westerly phase of QBO, respectively. While the underlying mechanism of the MJO-QBO relationship has remained elusive, one of the most popular hypotheses is that the weakened stability in the upper troposphere and lower stratosphere during easterly QBO years provides a preferable condition for deep convection to develop deeper and persist longer.

To test the stability hypothesis for the QBO control on the MJO, we examine properties of the convective aggregates of TCPRs in the southern Maritime Continent (SMC) region, in which the contrast in MJO activities between easterly and westerly QBO years is most pronounced. By taking advantage of TCPRs, we made composites domain mean properties (e.g., the total size of core and stratiform clouds, heaviness of precipitation, etc.), and core specific properties (e.g., top height and thickness, energy budget properties, etc.) for different phases of MJO and QBO, and the results are compared to find any systematic difference in the characteristics of convective aggregates. Our results provide practical evidences that enhanced stability due to temperature anomaly at lower stratosphere results in weaker convection in the SMC region, thus weakened eastward propagation of MJO.

REFERENCES

- Hendon, H. H., & Abhik, S. (2018). Differences in Vertical Structure of the Madden-Julian Oscillation Associated With the Quasi-Biennial Oscillation. *Geophysical Research Letters*, *45*(9), 4419–4428. <https://doi.org/10.1029/2018GL077207>
- Jin, D., Oreopoulos, L., Lee, D., Tan, J., & Cho, N. (2021). Cloud–Precipitation Hybrid Regimes and Their Projection onto IMERG Precipitation Data. *Journal of Applied Meteorology and Climatology*, *60*(6), 733–748. <https://doi.org/10.1175/JAMC-D-20-0253.1>
- Martin, Z., Orbe, C., Wang, S., & Sobel, A. (2021). The MJO-QBO Relationship in a GCM with Stratospheric Nudging. *Journal of Climate*, *34*(11), 1–69. <https://doi.org/10.1175/JCLI-D-20-0636.1>
- Nishimoto, E., & Yoden, S. (2017). Influence of the Stratospheric Quasi-Biennial Oscillation on the Madden–Julian Oscillation during Austral Summer. *Journal of the Atmospheric Sciences*, *74*(4), 1105–1125. <https://doi.org/10.1175/JAS-D-16-0205.1>
- Son, S.-W., Lim, Y., Yoo, C., Hendon, H. H., & Kim, J. (2017). Stratospheric Control of the Madden–Julian Oscillation. *Journal of Climate*, *30*(6), 1909–1922. <https://doi.org/10.1175/JCLI-D-16-0620.1>
- Yoo, C., & Son, S. (2016). Modulation of the boreal wintertime Madden-Julian oscillation by the stratospheric quasi-biennial oscillation. *Geophysical Research Letters*, *43*(3), 1392–1398. <https://doi.org/10.1002/2016GL067762>